

Comparing the T and π Equivalent Circuits for the Calculation of Transformer Inrush Currents

Francisco de León, *Senior Member, IEEE*, Ashkan Farazmand, and Pekir Joseph, *Student Member, IEEE*

Abstract—The most commonly used equivalent circuit for transformers is the traditional (Steinmetz) T -equivalent proposed toward the end of the 19th century. This model has two leakage impedance branches and one magnetizing branch. The T model properly represents the terminal behavior of the transformer for most low-frequency operating conditions. Another model derived from the principle of duality between magnetic and electric circuits exists, the π equivalent circuit, which has two magnetizing branches and one leakage branch. This paper shows that while the two equivalent circuits provide the same accuracy in steady state, better accuracy for the calculation of inrush currents is obtained with the π -equivalent circuit. Laboratory tests performed on three transformers with different characteristics demonstrate that inrush current simulations with the T equivalent circuit can have errors up to 73%, while the π equivalent estimates the measurements in every case within a few percent.

Index Terms—Duality, inrush currents, transformer equivalent circuits, transformer modeling.

I. INTRODUCTION

FOR LONGER than a century, the generally accepted equivalent circuit for a two-winding transformer has been the T equivalent. This model has the leakage inductance (L_s) divided into two branches—one is associated with the primary (L_{s1}) and the other is associated with the secondary winding (L_{s2}). The model is completed with a shunt magnetizing branch (composed by the parallel R_m, L_m); see Fig. 1. The originator of the equivalent circuit seems to be Steinmetz in 1897 [1]. A detailed discussion of the physical meaning of the elements of the T equivalent circuit is also given in [1].

As early as 1925, Boyajian [2] demonstrated the impossibility of a physically meaningful resolution of the leakage inductance as belonging partially to the primary winding and partially to the secondary winding (as is done in Fig. 1). The leakage inductance can only be defined (or measured) for a pair of windings. Therefore, the T equivalent circuit should be seen only as a terminal equivalent circuit since its elements do not have any physical relationship with the building components of a transformer (core and windings).

Cherry [3] in 1949 showed that equivalent circuits for transformers could be conveniently obtained from the principle of duality between magnetic and electric circuits. When duality is

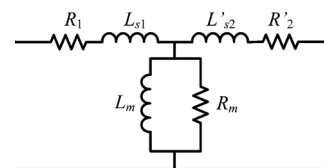


Fig. 1. T equivalent circuit.

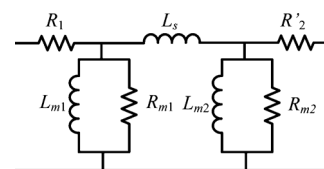


Fig. 2. π equivalent circuit.

applied to a single-phase transformer (both core and shell types), the obtained π model has only one leakage inductance branch in series and two shunt magnetizing branches (see Fig. 2). In 1951, Boyajian [4] discussed the benefits of the π equivalent circuit, emphasizing the unity of the leakage reactance between a pair of windings.

In 1953, Slemon [5] generalized the theory of duality and showed how nonlinearities can be introduced into the circuit elements of the π equivalent since they have a one-to-one relationship with the transformer flux paths. Duality-derived models have long been used for the calculation of electromagnetic transients [6]–[8]. However, they have not made the transition to steady state. The reason is perhaps that for steady-state studies (not involving heavy saturation), the T model gives almost perfect results. Moreover, for the most common power system studies such as: load flow, short circuit, and stability, the (shunt) magnetizing branch, whose impedance is normally very large when compared to the (series) leakage impedance, is often neglected. This renders the two circuits identical.

This paper shows, experimentally and analytically, that there are conditions where the T equivalent circuit is not capable of properly representing the transformer under heavy saturation conditions. For example, when a transformer has large leakage inductance and the core saturates, the T equivalent circuit fails to reproduce the terminal behavior. Errors in the order of 73% were measured with the T equivalent circuit in the inrush currents for transformers with relatively large leakage inductance.

To explain the reasons why the π model performs better than the T model, three existing transformers with different parameters were selected for the experimental study: 1) A standard transformer (T_s), which is characterized by typical leakage and magnetizing inductance values; 2) A standard

Manuscript received April 28, 2012; accepted July 06, 2012. Date of publication August 27, 2012; date of current version September 19, 2012. Paper no. TPWRD-00437-2012.

The authors are with the Department of Electrical and Computer Engineering, Polytechnic University, Brooklyn, NY 11201 USA (e-mail: fdeleon@poly.edu; afaraz01@students.poly.edu; pekirj@yahoo.com).

Color versions of one or more of the figures in this paper are available online at <http://ieeexplore.ieee.org>.

Digital Object Identifier 10.1109/TPWRD.2012.2208229

toroidal transformer (T_T), which is characterized by having large magnetizing inductance and very small leakage inductance; 3) A second toroidal transformer (T_L) designed with no overlapping sectored windings of 180° . This produces a very large leakage inductance. The geometrical information is given in Table VIII.

In the next section, the parameters of the equivalent circuit for each transformer are measured and compared. In Section III, the air-core inductance, essential for the proper calculation of inrush currents, is computed with 3-D finite-elements simulations. In Section IV, the inrush performance of the two models is compared. In Section V, a parametric analysis on how the division of the leakage and magnetizing inductances affect the transformer inrush current is presented. Finally, in Section VI, the large errors obtained with the T model are explained by analyzing the variation of the open-circuit impedance as the core saturates and the leakage inductance increases.

II. PARAMETER MEASUREMENT

Accurate determination of the transformer magnetizing and leakage parameters is of paramount importance to produce a correct comparison of model performance. To determine the parameters, the procedures of the IEEE Standard C57.12.91-1995 [9] for open-circuit and impedance tests were followed. The measurements of instantaneous voltage and current are obtained very precisely using a YOKOGAWA 2-MHz power analyzer (PZ4000), with a sampling rate of 20 μ s. From the measuring system, 833 samples per cycle of voltage and current are obtained. The rms values for voltage and current are computed from basic principles as follows:

$$\begin{aligned} v_{\text{rms}} &= \sqrt{\frac{1}{T} \int_0^T v^2(t) dt}; \\ i_{\text{rms}} &= \sqrt{\frac{1}{T} \int_0^T i^2(t) dt}. \end{aligned} \quad (1)$$

The active power is computed from the average of the instantaneous power as

$$P = \frac{1}{T} \int_0^T v(t) i(t) dt. \quad (2)$$

The reactive power is calculated with the following formula:

$$Q = \sqrt{(v_{\text{rms}} i_{\text{rms}})^2 - P^2}. \quad (3)$$

A. Open-Circuit Test

The low-voltage (LV) winding of the transformer is energized with rated voltage, keeping the high-voltage (HV) side in open circuit. The terminal voltage of the HV (open) side and current of the LV (connected) side are captured.

B. Impedance Test

The HV winding is energized with the LV winding short-circuited. The voltage applied is varied from 4% to 20% of the rated voltage to obtain the rated current in the LV winding (see Table I).

TABLE I
RESULTS OF THE STANDARDIZED TESTS ON THE THREE TRANSFORMERS

Transformer	T_S Standard Leakage	T_T Reduced Leakage	T_L Enlarged Leakage
V_{oc} [V]	120.18	120.04	120.19
I_{oc} [A]	5.3297	0.30886	0.254976
P_{oc} [W]	39.08	10.18	13.44
Ratio	1:1	1:1	1:1
Rating [kVA]	1	1	1
V_{sc} [V]	5.15	5.08	24.73
I_{sc} [A]	8.38	8.73	8.75
P_{sc} [W]	40.351	43.9859	46.871

C. Calculation of Circuit Parameters

Table I shows the results of the standardized open-circuit (oc) and impedance or short-circuit (sc) tests (at 60 Hz) for the three transformers under study. The parameters of the equivalent circuits are computed with the following expressions:

$$R_1 + R_2' = \frac{P_{sc}}{I_{sc}^2} \quad (4a)$$

$$L_s = \frac{1}{2\pi f} \sqrt{\left(\frac{V_{sc}}{I_{sc}}\right)^2 - (R_1 + R_2')^2} \quad (4b)$$

$$\begin{aligned} R_m &= \frac{(V_{oc} - R_1 I_{oc})^2}{P_{oc}}; \\ L_m &= \frac{(V_{oc} - R_1 I_{oc})^2}{2\pi f Q_{oc}} \end{aligned} \quad (5)$$

where P_{sc} and P_{oc} are the active powers computed from the short-circuit and open-circuit tests, respectively. Q_{oc} is the open-circuit reactive power. V_{sc} and I_{sc} are the rms values of short-circuit voltages and currents, respectively. V_{oc} and I_{oc} are the rms values of open-circuit voltages and currents, respectively. L_s is the total (series) leakage inductance. R_m is the magnetizing resistance, L_m is the magnetizing inductance, R_1 and R_2 are the primary and the secondary ac resistances, respectively, and $f = 60$ Hz.

The total series ac resistance $R_1 + R_2'$ is computed from (4a). Individual breakdown of the resistances is needed for the equivalent models. In addition, primary and secondary leakage inductances are also needed for the T model. When no information is given on the value of the individual dc resistances, dividing the leakage (and ac resistance) equally into the two windings [10] is accepted. For this paper, measurement of the dc resistance was performed. Therefore, the leakage inductance and ac resistance are divided into two as it is traditionally done in proportion to the dc resistances [11]; see Table II. In Section V, this division of the leakage impedance is varied over a wide range to gauge the effect of having more or less leakage to each side. The magnetizing parameters of the T model are obtained directly from (5).

For the π model, the leakage inductance is obtained directly from (4b), and the magnetizing parameters are the double of

TABLE II
CIRCUIT PARAMETERS FOR T AND π MODELS

Transformer	T_S Standard Leakage	T_T Reduced Leakage	T_L Enlarged Leakage
R_1 [Ω]	0.251	0.277	0.306
R'_2 [Ω]	0.324	0.300	0.305
L_{s1} [mH]	0.302	0.111	4.393
L'_{s2} [mH]	0.390	0.121	4.385
R_m [Ω]	369.53	1,415.97	1,074.71
L_m [mH]	71.91	1,284.73	1,669.60
L_s [mH]	0.692	0.232	8.778
R_{m1} [Ω]	739.06	2,831.94	2,149.42
R_{m2} [Ω]	739.06	2,831.94	2,149.42
L_{m1} [mH]	143.82	2,569.46	3,339.21
L_{m2} [mH]	143.82	2,569.46	3,339.21
L_m/L_s	103.89	5,537.63	190.20

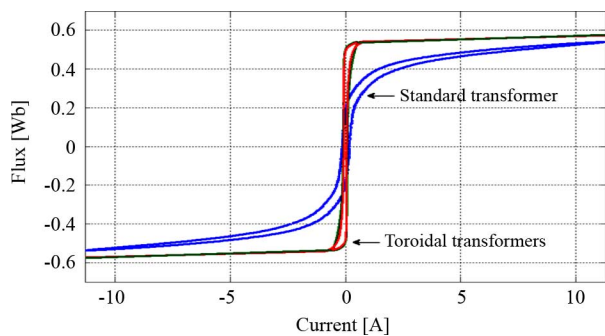


Fig. 3. Hysteresis cycles of the transformers T_S (standard design), T_T (reduced leakage), and T_L (enlarged leakage).

those obtained from (5)[8]. Therefore, $R_{m1} = R_{m2} = 2R_m$ and $L_{m1} = L_{m2} = 2L_m$. Also, in Section V, this division of the magnetizing impedance is varied over a wide range to determine the effect of assigning more or less magnetization to each side. The parameters computed from rated measurements are shown in Table II.

D. Hysteresis Cycles

A family of hysteresis curves was obtained for each of the three transformers under test. These hysteresis curves are acquired from the measurement of the instantaneous values of voltage and current. Faraday's Law is then used to convert the induced voltage into flux. The hysteresis cycles of transformers T_S , T_T , and T_L are shown in Fig. 3. In Appendix B, the numerical values of the upper part of the cycles are given (as required by the EMTP-RV [12]).

One can appreciate from Fig. 3 that the standard transformer (T_S) shows traditional hysteresis cycles. The toroidal transformers (T_T and T_L) have flat and narrow hysteresis cycles. This is so because there are no gaps in the core. Fig. 4 shows a zoom on the hysteresis cycles of the toroidal transformers. Note that the transformer with enlarged leakage T_L has a slightly wider cycle, but the saturation flux is the same.

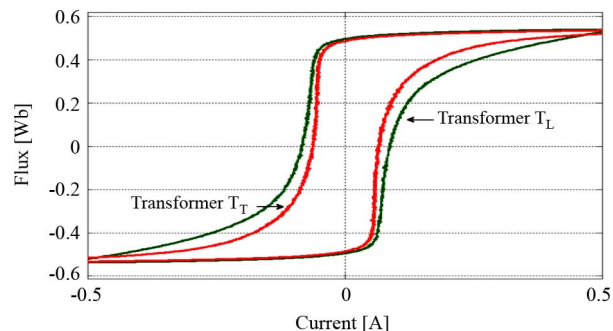


Fig. 4. Hysteresis cycles of the toroidal transformers (T_T and T_L).

TABLE III
AIR-CORE INDUCTANCE FOR THE TRANSFORMERS

Transformer	T_S Standard Leakage	T_T Reduced Leakage	T_L Enlarged Leakage
Air-core Inductance	1000 [μ H]	316 [μ H]	463 [μ H]

III. AIR-CORE INDUCTANCES

It was not possible to measure the deep saturation section region of the hysteresis loops in the lab due to the large power requirements (high voltage and high current). Yet, this region is of paramount importance to properly compute the inrush currents. 3-D finite element (FEM) simulations were performed to determine the air-core inductance. The commercial program COMSOL Multiphysics was used for this purpose [13]; see Appendix A.

The dimensions of the LV winding were used for the finite-element method (FEM) simulations using air cores. The volume magnetic energy is extracted directly from COMSOL and then the inductance is calculated using the following formula:

$$L_{\text{air-core}} = \frac{2W}{I^2}. \quad (6)$$

Table III gives the air-core inductances of the three transformers studied in this paper. Note, however, that the construction details of the standard transformer T_S are not known. Therefore, an estimation was obtained from the inrush tests. The hysteresis curve is extended using the air-core inductances as the slope from the last measured point to infinity. These values are included in the tables of Appendix B.

IV. MODEL COMPARISON

A. Description of the Inrush Current Experiments

Starting with the transformer core demagnetized, the worst conditions (maximum inrush currents) occur when the energization coincides with the voltage-wave zero crossing [14]. This situation can be reproduced in the laboratory by connecting the transformer through a zero-crossing detecting switch as shown in Fig. 5. To obtain accurate and consistent inrush current measurements, any remanence in the transformer from the previous energization must be removed [15]. The remanence removal

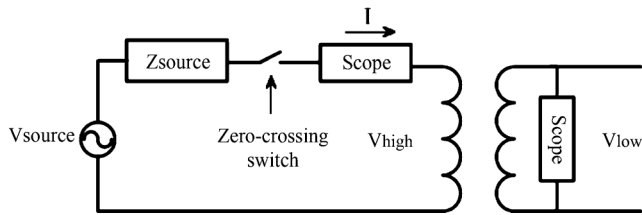


Fig. 5. Model of the experimental setup for measuring inrush currents.

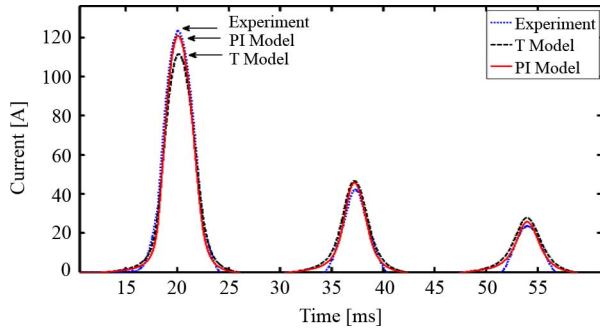


Fig. 6. Inrush current comparison: Experimental versus simulated results using T and π models for transformer T_S (standard design).

process was done by gradually reducing the voltage to zero before de-energizing the transformer from the source.

A zero-crossing switch consisting of voltage regulators, optic isolators, digital-logic control circuits, and metal-oxide field-effect transistors (MOSFETs) is used to switch-on the transformer. When the source voltage crosses zero, the switch is closed and the waveforms of inrush current are captured with the power analyzer. The results are compared with simulations in the next section.

B. Simulations Versus Measurements

The EMTP-RV [12] was used for the simulation of the tests described in Fig. 5 using the two equivalent circuits (Figs. 1 and 2). The nonlinear characteristics of all inductors representing iron-core components are modeled with the built-in hysteresis fitter (using the data computed in the previous section). The short-circuit impedance of the source was measured, which is almost purely resistive with a value of $Z_{source} = 0.1444 \Omega$. Figs. 6–8 compare the results obtained by simulation using the T and π models against the measurements for the three transformers under study.

Fig. 6 shows the results for the standard transformer T_S . The peak value of the inrush current using the π model is 121.1 A, which is very close to the experiment result (123.7 A). In this case, the difference is only 2%, while the T model gives 111.7 A, which corresponds to 10% difference with respect to the experiment result. The current shape of both models follows the same path for low currents and only toward the peak they separate. The peak of the measured inrush current is about 10 times larger than the rated 11.78 A peak (8.33 A rms).

Fig. 7 shows the results for the toroidal transformer T_T , whose main characteristics are to have very small leakage inductance and very large magnetizing inductance (see Table II).

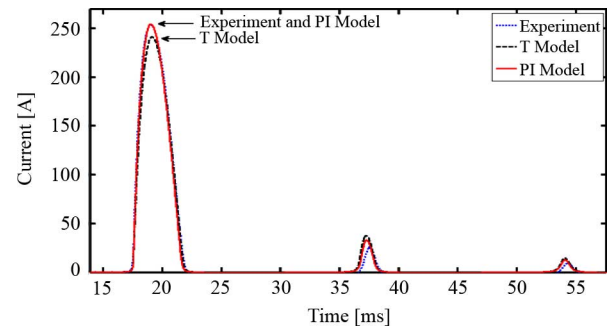


Fig. 7. Inrush current comparison: Experimental versus simulated results using T and π models for transformer T_T (very small leakage inductance).

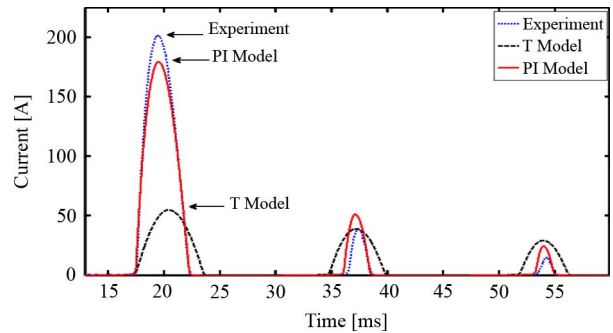


Fig. 8. Inrush current comparison: Experimental versus simulated results using T and π models for transformer T_L (very large leakage inductance).

The π model and experiment give the same value for the first peak (254.5 A), while the T model shows 241.4 A. In this case for the T model, the difference is about 5% at the peak with the experiment result. For this transformer, the measured inrush current is about 22 times larger than the rated current.

Fig. 8 shows the results for the toroidal sector wound transformer T_L , whose main features are to have a very large leakage inductance and a very large magnetizing inductance (see Table II). In this case, the measured peak of the inrush current is 201.4 A peak (about 17 times larger than the rated current).

The π model gives 179.4 A at the first peak, which represents a difference of 10.9% with respect to the experiment result, while the T model yields 54.9 A, which corresponds to a very large error of 72.7% at the peak.

Note that the measured peak inrush current of transformer T_T is about 26% larger than the peak inrush current of transformer T_L . This is because of the larger leakage inductance value of the transformer T_L in comparison to T_T (almost 38 times) which limits the inrush current considerably.

For all three transformers, the π model gives more precise results than the T model. When the leakage inductance is small (transformers T_T and T_S), the T model results are also acceptable and relatively close to the experiment, but when the leakage inductance is large (transformer T_L), the T and π models behave quite differently: the T model shows very large error, while the π model is close to the experimental results.

From the results of the simulations and measurements of this section, one can conclude that model selection plays an impor-

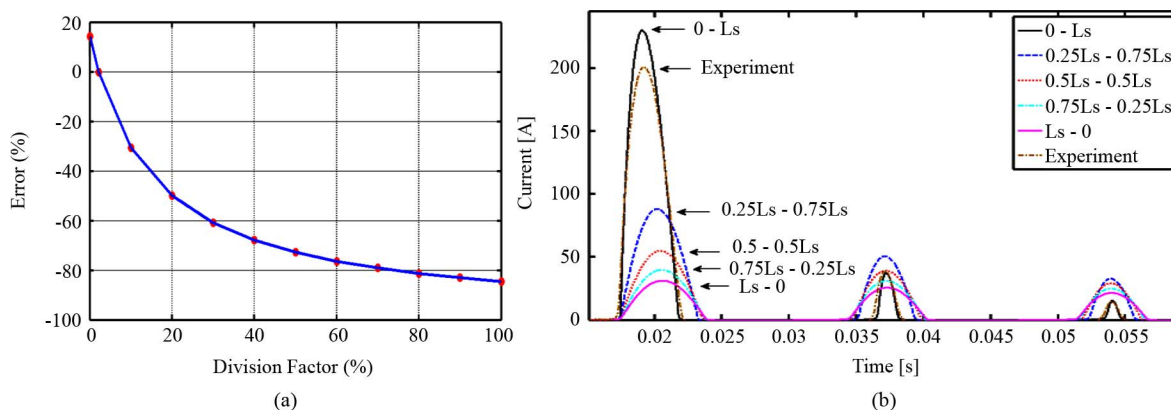


Fig. 9. Inrush current comparison using the T model for transformer T_L under different division factors for the leakage inductance. (a) Error with respect to the experiment. (b) Inrush current waveforms.

tant role in the calculation of inrush currents when the leakage inductance is large. We make the statement that the π model should be always used, not only because its elements have a clear physical meaning, but also because large errors may appear when using the traditional T model. Both circuits are very simple, the π model has only one more circuit element (7 versus 6) than the T model, but the π equivalent may provide better results under heavy saturation conditions.

V. PARAMETRIC STUDIES

In this section, a parametric analysis of how the division of the leakage and magnetizing inductances affect the calculated inrush currents using the T and π models is presented.

Transformer T_L has been selected to illustrate the parametric simulations because this is the one that presents larger variations; see Table IV. The first column presents a division factor a used to split the total leakage inductance (L_s) into primary and secondary sides of the T model. For example, the first row (corresponding to $a = 0$) presents the case when all leakage inductance is entirely on the secondary side of the T model. In the next row ($a = 10\%$), 10% of the leakage is placed on the primary side and 90% on the secondary side. In the last case ($a = 100\%$), all of the leakage inductance is on the primary side of the transformer.

The last column of Table IV presents the errors in the calculated peak currents between the T model and the experimental results. From the results, it is obvious that increasing the primary side leakage (L_{s1}) limits the inrush current considerably, which causes large errors. For the case in which the division factor is 50% [10], the error is 71.97%; when the leakage inductance is divided based on the dc resistances (as recommended in [11]), the error is 72.7%; and the error is zero when only 2.7% of the total leakage inductance is on the primary side of the transformer. Fig. 9 compares the inrush current waveforms for five different cases using a 25% division factor. From the figure, one can observe that the inrush current computed with the T model shows large sensitivity, especially at the beginning.

To study the splitting of the magnetizing impedance in the π model, a division factor of 25% has been selected. The total magnetizing current between the two magnetizing branches is

TABLE IV
PARAMETRIC STUDY OF T MODEL (LEAKAGE INDUCTANCE DIVISION)

a (%)	L_{s1} [mH]	L_{s2} [mH]	Peak Current [A]	Error [%]
0	0.000	8.778	230.36	14.38
10	0.878	7.900	139.75	-30.61
20	1.756	7.022	100.72	-49.99
30	2.633	6.145	78.83	-60.86
40	3.511	5.267	64.78	-67.84
50	4.389	4.389	54.99	-72.70
60	5.267	3.511	47.78	-76.28
70	6.145	2.633	42.24	-79.03
80	7.022	1.756	37.86	-81.20
90	7.900	0.878	34.3	-82.97
100	8.778	0.000	31.35	-84.43
Case with zero error:				
2.2	0.192	8.586	201.4	0.00

TABLE V
PARAMETRIC STUDY OF THE π MODEL (MAGNETIZING INDUCTANCE DIVISION)

a (%)	Peak Current [A]	Error [%]
0	230.3	14.38
25	211.3	4.92
50	179.4	-10.92
75	128.2	-36.35
100	31.34	-84.43
Case with zero error:		
32.5	201.4	0.00

divided proportionally. Remember that the magnetizing model is nonlinear since it includes saturation and hysteresis. As shown in Table V, the first and last cases (with division factors of 0 and 100%, respectively) are equal to the cases with one magnetizing branch. Therefore, for these two cases, the results are exactly the same as the first and last cases of the T model (see Table IV).

In all other cases, the error is smaller than for the T model. The error is zero when the division factor is about 32.5%, and for a 50% division factor, the error is 10.9% (as presented in Section IV). Fig. 10 compares the inrush current waveforms for the different cases with the experiment result. Analyzing Figs. 9 and 10, one can see that the calculations are less sensitive to the division factor in the π model than in the T model.

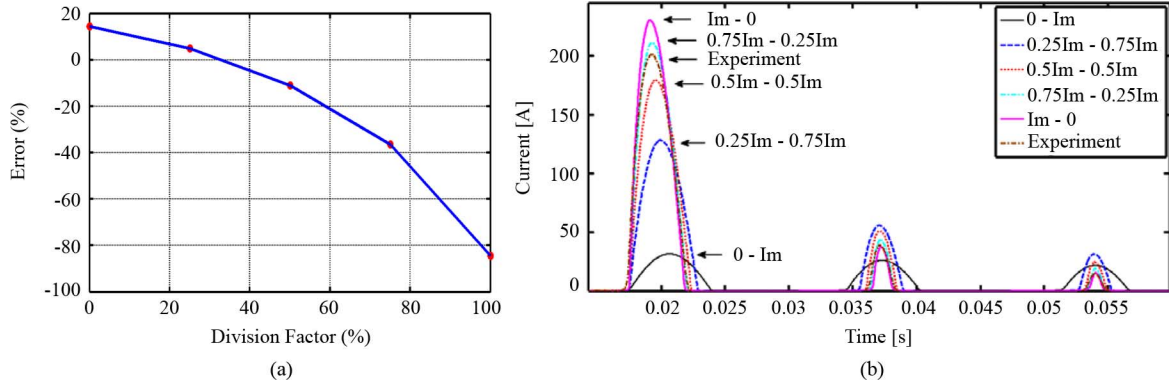


Fig. 10. Inrush current comparison using the π model for transformer T_L , under different division factors for the magnetizing impedance. (a) Error with respect to the experiment. (b) Inrush current waveforms.

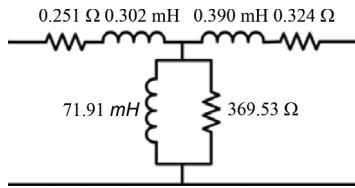


Fig. 11. T equivalent circuit for the transformer T_L at nominal voltage.

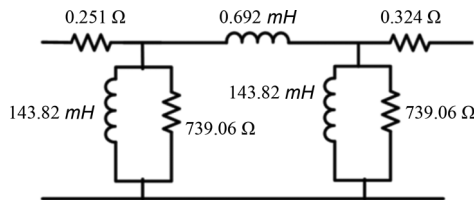


Fig. 12. π equivalent circuit for the transformer T_L at nominal voltage.

VI. ANALYSIS OF THE TERMINAL IMPEDANCE

In this section, the large errors obtained with the T model are explained by analyzing the variation of the open-circuit impedance as the core saturates (L_m reduces). In addition, the effect of increasing the leakage inductance (L_s) is presented. The (open circuit) equivalent impedance for the T and π equivalent circuits can be computed from series-parallel simplifications of the circuits of Figs. 1 and 2, respectively, as follows:

$$Z_T = R_1 + j\omega L_{s1} + \frac{1}{\frac{1}{R_m} + \frac{1}{j\omega L_m}} \quad (7)$$

$$Z_\pi = R_1 + \frac{1}{\frac{1}{R_{m1}} + \frac{1}{j\omega L_{m1}} + \frac{1}{j\omega L_s + \frac{1}{\frac{1}{R_{m2}} + \frac{1}{j\omega L_{m2}}}}} \quad (8)$$

Using the values for the enlarged leakage transformer (T_L) from the first column of Table II, we find the equivalent circuits of Figs. 11 and 12

The effect of increasing the leakage inductance on the terminal impedance is studied by varying the parameters of the equivalent circuits of Figs. 11 and 12. The leakage inductances L_s , together with L_{s1} and L_{s2} , were increased (one thousand times) in small steps. Fig. 13 shows the terminal (open circuit) impedance for the T and π models against the leakage

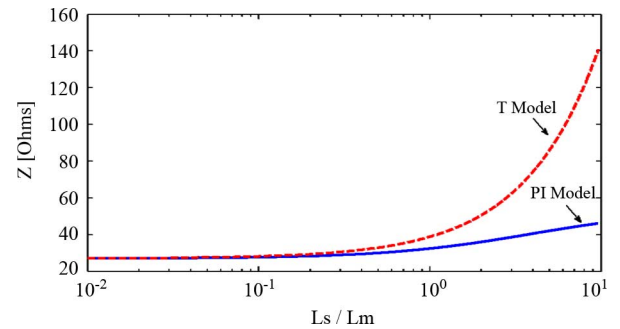


Fig. 13. Variation of the terminal (open circuit) impedance with respect to the ratio of leakage versus magnetizing inductances increasing the leakage inductance.

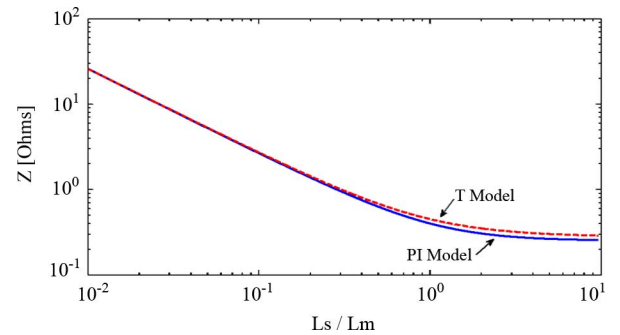


Fig. 14. Variation of the terminal (open circuit) impedance with respect to the ratio of leakage versus magnetizing inductances reducing the magnetizing inductance.

inductance (normalized with the magnetizing inductance L_m). One can see that for small L_s/L_m ratios, both circuits give the same terminal impedance. This is the normal region because $L_m \gg L_s$ for most transformers. However, as the ratio L_s/L_m increases, the impedance of the T model increases much faster than the impedance of the π model. Under heavy saturation conditions, L_m is small. This explains why the T model underestimates the inrush currents for transformers with large leakage inductance (see Fig. 8).

To study the effect on the open-circuit impedance of the reduction of the magnetizing inductance due to saturation, L_m , together with $L_{m1} = L_{m2} = 2L_m$, were decreased in small steps to a value of 1000 times smaller. The terminal impedance calculations (shown in Fig. 14) indicate that the saturation of the core,

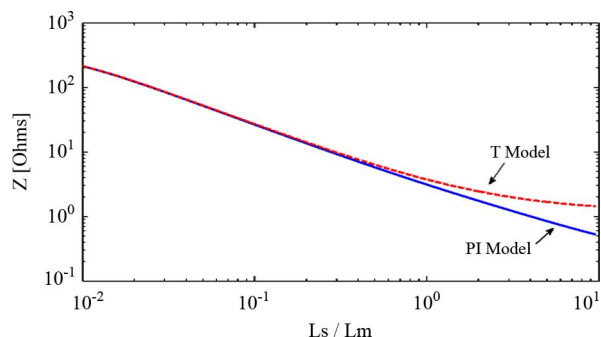


Fig. 15. Variation of the terminal (open circuit) impedance with respect to the ratio of leakage versus magnetizing inductances for an increased leakage inductance transformer.

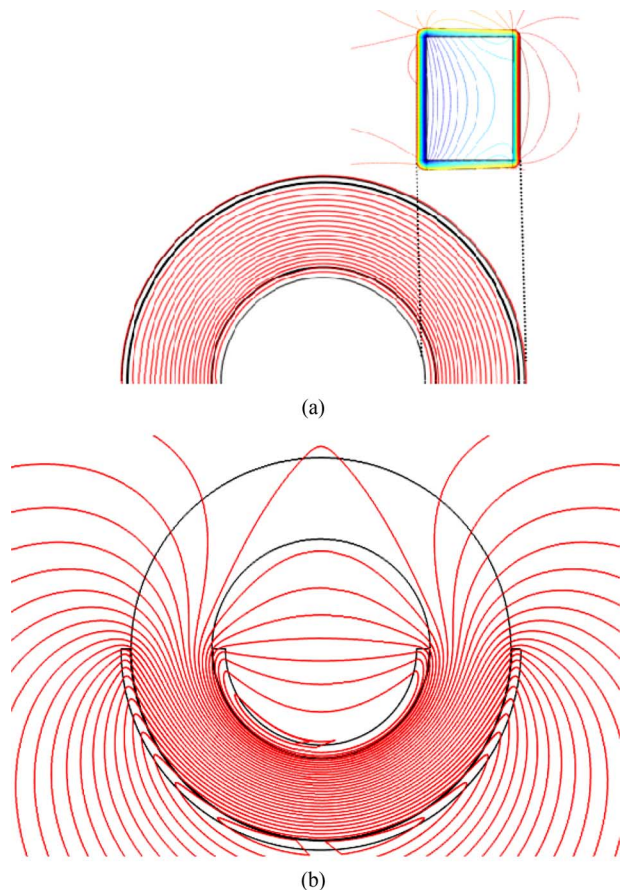


Fig. 16. (a) Magnetic flux density for the transformer T_T . (b) Magnetic flux density for the transformer T_L .

by itself, is not responsible for the large terminal impedance differences between the T and π models. When the leakage inductance of the transformer is increased 10 times from 0.692 to 6.92 mH, the impedance variation of Fig. 15 is obtained. Small differences exist when the magnetizing inductance is large (not saturated), but larger differences can be observed when the magnetizing inductance is small (saturated).

The results of this section explain why both models give about the same inrush current for transformers with small leakage inductance; see Figs. 6 and 7. Looking at the topology of the two circuits (Figs. 11 and 12), one can observe that in the T model, the primary winding leakage inductance (L_{S1}) limits the circulation of current to the magnetizing branch. This prevents large

TABLE VI
NUMERICAL VALUES OF THE HYSTERESIS
CYCLE OF TRANSFORMERS (T-MODEL)

T_S (Standard Leakage)		T_T (Reduced Leakage)		T_L (Enlarged Leakage)	
I [A]	Flux [Wb]	I [A]	Flux [Wb]	I [A]	Flux [Wb]
0.1873	0	0.0598	0	0.0992	0
0.2025	0.0351	0.0714	0.0619	0.1024	0.0323
0.2739	0.1030	0.0793	0.1823	0.1119	0.0955
0.3148	0.1366	0.0897	0.2115	0.1224	0.1269
0.4082	0.1700	0.1031	0.2683	0.1258	0.1579
0.5248	0.2030	0.1117	0.2958	0.1334	0.1886
0.7024	0.2354	0.1312	0.3226	0.1463	0.2188
0.9172	0.2673	0.1520	0.3485	0.1647	0.2485
1.1522	0.2986	0.1593	0.3736	0.1781	0.2775
1.4849	0.3291	0.1978	0.3978	0.2030	0.3059
1.9048	0.3588	0.2283	0.4210	0.2301	0.3335
3.3269	0.4153	0.3082	0.4641	0.3009	0.3860
4.4774	0.4420	0.3906	0.4840	0.3492	0.4108
6.0106	0.4675	0.4938	0.5026	0.4059	0.4346
8.0034	0.4918	0.6799	0.5201	0.4767	0.4573
10.2941	0.5147	0.9827	0.5362	0.5560	0.4787
12.7635	0.5362	1.5833	0.5509	0.6588	0.4989
15.2251	0.5562	2.8455	0.5641	0.7828	0.5177
17.7922	0.5749	5.1459	0.5758	0.9642	0.5351
20.3166	0.5920	9.6796	0.5859	1.2713	0.5506
22.7446	0.6074	17.9407	0.5941	1.8412	0.5636
25.0224	0.6213	29.6356	0.6002	2.8446	0.5739
27.2454	0.6335	40.0726	0.6042	4.6666	0.5816
29.3236	0.6440	45.7422	0.6062	8.2994	0.5872
30.6528	31.2725	46.8378	0.6066	15.2306	0.5912
33.0559	0.6600	600	0.7814	23.6656	0.5937
34.5354	0.6653			30.3695	0.5952
35.6353	0.6690			34.4554	0.5960
36.1479	0.6709			35.8700	0.5962
400	1.0348			600	0.8574

currents (especially inrush when the core saturates) to be drawn by the transformer. In the π model, the path of the inrush current is open to one of the magnetizing branches. Therefore, in this case, the π model is more precise than the T model (see Fig. 8).

VII. CONCLUSION

This paper has shown experimentally that the traditional T model of transformers may yield large errors when computing inrush currents. This is especially true when the transformers have large leakage inductance. Better accuracy for the calculation of inrush currents has been obtained with the π equivalent circuit. Laboratory tests performed on several transformers demonstrate that inrush current simulations with the T equivalent circuit could under predict the inrush currents by as much as 72.7%, while the π equivalent circuit predicts the measurements with a small percent error.

Physical, numerical, and analytical explanations on the performance difference of the two models were given. The topology of the T model, having the primary winding leakage inductance element before a magnetizing branch, is the cause for the model inaccuracies since it (incorrectly) limits the circulation of current to the magnetizing branch when the core saturates.

APPENDIX A AIR-CORE INDUCTANCE

Since it was not possible to measure the air-core inductance in the lab because of the high-power requirements, 3-D finite-element simulations were performed. Fig. 16(a) and (b) shows

TABLE VII
NUMERICAL VALUES OF THE HYSTERESIS
CYCLE OF TRANSFORMERS (PI-MODEL)

T_S (Standard Leakage)		T_T (Reduced Leakage)		T_L (Enlarged Leakage)	
I [A]	Flux [Wb]	I [A]	Flux [Wb]	I [A]	Flux [Wb]
0.0936	0	0.0299	0	0.0496	0
0.1013	0.0351	0.0357	0.0619	0.0512	0.0323
0.1370	0.1030	0.0397	0.1823	0.0560	0.0955
0.1574	0.1366	0.0449	0.2115	0.0612	0.1269
0.2041	0.1700	0.0516	0.2683	0.0629	0.1579
0.2624	0.2030	0.0558	0.2958	0.0667	0.1886
0.3512	0.2354	0.0656	0.3226	0.0732	0.2188
0.4586	0.2673	0.0760	0.3485	0.0823	0.2485
0.5761	0.2986	0.0797	0.3736	0.0890	0.2775
0.7424	0.3291	0.0989	0.3978	0.1015	0.3059
0.9524	0.3588	0.1141	0.4210	0.1150	0.3335
1.6635	0.4153	0.1541	0.4641	0.1504	0.3860
2.2387	0.4420	0.1953	0.4840	0.1746	0.4108
3.0053	0.4675	0.2469	0.5026	0.2029	0.4346
4.0017	0.4918	0.3400	0.5201	0.2383	0.4573
5.1470	0.5147	0.4913	0.5362	0.2780	0.4787
6.3818	0.5362	0.7916	0.5509	0.3294	0.4989
7.6126	0.5562	1.4227	0.5641	0.3914	0.5177
8.8961	0.5749	2.5729	0.5758	0.4821	0.5351
10.1583	0.5920	4.8398	0.5859	0.6357	0.5506
11.3723	0.6074	8.9703	0.5941	0.9206	0.5636
12.5112	0.6213	14.8178	0.6002	1.4223	0.5739
13.6227	0.6335	20.0363	0.6042	2.3333	0.5816
14.6618	0.6440	22.8711	0.6062	4.1497	0.5872
15.6362	0.6528	23.4189	0.6066	7.6153	0.5912
16.5280	0.6600	300	0.7814	11.8328	0.5937
17.2677	0.6653			15.1848	0.5952
17.8176	0.6690			17.2277	0.5960
18.0740	0.6709			17.9350	0.5962
200	1.0348			300	0.8574

TABLE VIII
CONSTRUCTION INFORMATION OF THE TOROIDAL TRANSFORMERS UNDER
TEST

Core Dimensions [inches]			Winding Characteristics			
Internal Diameter	Outer Diameter	Height	Primary winding		Secondary winding	
			Number of Turns	Wire gauge	Number of Turns	Wire gauge
3.375	5.875	2	196	13	196	13

the top view of the distribution of the magnetic flux density for the T_T and T_L transformers, respectively. Transformer T_T has the winding distributed over the entire 360° , while transformer T_L occupies only 180° . From Fig. 16(a), one can see that the field is mostly contained inside the coil with higher flux densities toward the inner diameter. Fig. 16(b) shows that for the T_L transformer, the flux density is concentrated inside the wound semicircle, but the return through the air is quite scattered.

APPENDIX B VALUES OF THE HYSTERESIS CYCLES

Tables VI and VII present the numerical values of the hysteresis cycles used for the T and π models for the three transformers. Note that because the π model has two shunt inductors, the value of the current is half for the same flux.

ACKNOWLEDGMENT

The authors would like to express their gratitude to R. Kumar and X. Xu, both ex-graduate students of New York University-Poly, for their help during the initial experimental stages of this project. They would also like to thank B. Kovan, current graduate student of New York University-Poly, for performing the finite-element simulations to compute the air-core inductance. The efforts of N. Augustine with the finite-element simulations are also recognized. K. Zhang has built the zero crossing switch used in the experiments.

REFERENCES

- [1] C. P. Steinmetz, *Theory and Calculation of Alternating Current Phenomena* First Edition Available Through Open Library McGraw, 1897. [Online]. Available: <http://openlibrary.org>
- [2] A. Boyajian, "Resolution of transformer reactances into primary and secondary reactances," *AIEE Trans.*, pp. 805–810, Jun. 1925.
- [3] E. C. Cherry, "The duality between interlinked electric and magnetic circuits and the formation of transformer equivalent circuits," *Proc. Phys. Soc.*, vol. (B) 62, pp. 101–111, Feb. 1949.
- [4] L. F. Blume, A. Boyajian, G. Camilli, T. C. Lenox, S. Minneci, and V. M. Montsinger, *Transformer Engineering: A Treatise on the Theory, Operation, and Application of Transformers*. New York: Wiley, 1951, p. 70.
- [5] G. R. Slemmon, "Equivalent circuits for transformers and machines including nonlinear effects," *Proc. Inst. Elect. Eng.*, IV, vol. 100, pp. 129–143, 1953.
- [6] F. de León and A. Semlyen, "Complete transformer model for electromagnetic transients," *IEEE Trans. Power Del.*, vol. 9, no. 1, pp. 231–239, Jan. 1994.
- [7] J. A. Martinez and B. Mork, "Transformer modeling for low- and mid-frequency transients—A review," *IEEE Trans. Power Del.*, vol. 20, no. 2, pt. 2, pp. 1525–1632, Apr. 2005.
- [8] F. de León, P. Gómez, J. A. Martinez-Velasco, and M. Rioual, *Transformers in Power System Transients: Parameter Determination*, J. Martinez-Velasco, Ed. Boca Raton, FL: CRC, 2009, ch. 4, pp. 177–250.
- [9] *IEEE Standard Test Code for Dry-Type Distribution and Power Transformers, Recognized as an American National Standard (ANSI)*, IEEE Standard C57.12.91-1995, 1995.
- [10] V. Del Toro, *Principles of Electrical Engineering*, 2nd ed. Englewood Cliffs, NJ: Prentice-Hall, 1972.
- [11] *Staff of the Department of Electrical Engineering of Massachusetts Institute of Technology, Magnetic Circuits and Transformers*. New York: Wiley, 1943.
- [12] "DCG-EMTP (Development coordination group of EMTP) Version EMTP-RV, Electromagnetic Transients Program," [Online]. Available: <http://www.emtp.com>
- [13] "Comsol Multiphysics 4.2a User's Guide," Comsol, Inc., 2011.
- [14] A. Greenwood, *Electrical Transients in Power Systems*, 2nd ed. New York: Wiley, 1991, pp. 113–116.
- [15] B. Kovan, F. de León, D. Czarkowski, Z. Zabar, and L. Birenbaum, "Mitigation of inrush currents in network transformers by reducing the residual flux with an ultra-low-frequency power source," *IEEE Trans. Power Del.*, vol. 26, no. 3, pp. 1563–1570, Jul. 2011.

Francisco de León (S'86–M'92–SM'02) received the B.Sc. and M.Sc. (Hons.) degrees in electrical engineering from the National Polytechnic Institute, Mexico City, Mexico, in 1983 and 1986, respectively, and the Ph.D. degree from the University of Toronto, Toronto, ON, Canada, in 1992.

He has held several academic positions in Mexico and has worked for the Canadian electric industry. Currently, he is an Associate Professor at Polytechnic Institute of New York University (NYU), Brooklyn, NY. His research interests include the analysis of power phenomena under nonsinusoidal conditions, the transient and steady-state analyses of power systems, the thermal rating of cables, and the calculation of electromagnetic fields applied to machine design and modeling.

Ashkan Farzmand was born in Tehran, Iran, in 1983. He received the M.Sc. (Hons.) degree in electrical engineering from the University of Tehran, Tehran, Iran, in 2009, and is currently pursuing the Ph.D. degree in electrical engineering at the Polytechnic Institute of New York University, Brooklyn, NY.

His research interests are the design and analysis of transformers, electrical transients, derating of electrical machines under nonsinusoidal and unbalanced conditions, and power quality.

Pekir Joseph (S'09) was born in Brooklyn, NY, in 1987. He received the B.Sc. degree in electrical engineering and the M.Sc. degree in power system engineering from the Polytechnic Institute of New York University, Brooklyn, NY, in 2009 and 2011, respectively.

His research interests are in electrical transients, switching surges, relay protection and coordination, transmission and distribution, and inrush currents in transformers.